Susceptibility spectrum and parametric generation in an atomic vapor in a resonant light field

I. S. Zeĭlikovich, S. A. Pul'kin, L. S. Gaĭda, and V. N. Komar

Grodniensk State University
(Submitted 7 April 1988)
Zh. Eksp. Teor. Fiz. **94**, 76–89 (December 1988)

The absorption spectra of two-level atoms in mono- and bichromatic pump fields and three-level atoms in a monochromatic pump field are investigated theoretically and experimentally. The amplification of Stokes and anti-Stokes waves propagating in a nonlinear medium are examined. Parametric generation is achieved by placing sodium or barium atoms in the cavity of a one- or two-frequency dye laser. In the case of barium in a bichromatic pump, generation is achieved for a symmetric detuning of the pump frequencies from the resonant transmission frequency.

1. INTRODUCTION

It has been shown theoretically[1-3] that a resonant radiation field can produce significant changes in both absorption and emission line profiles of a two-level system. It was predicted[1] that the absorption coefficient for probe radiation should change sign, i.e., the radiation should be amplified even in the absence of a population inversion. The theory of the density matrix was used[4-7] to calculate the susceptibility spectrum of a two-level system, taking into account different longitudinal and transverse relaxation times. It was shown that the appearance of regions of amplification without inversion was due to stimulated three-photon Raman scattering of a resonant light wave. The phenomenon of amplification without population inversion in a two-level system was first discovered experimentally in the radiofrequency part of the spectrum.[8] A comparison between the theoretical and experimental behavior of susceptibility in the radiofrequency range during transitions between the hyperfine structure components of cadmium (^{111}Cd) was given in Ref. 9. The effect was investigated[10] in the optical range in a beam of sodium atoms, using transitions between hyperfine structure components. In our previous paper,[11] we investigated the frequency dependence of susceptibility (absorption and refractive index spectra) of an atomic system placed in the cavity of a dye laser.

Four-wave parametric amplification was predicted theoretically in Ref. 12 and observed experimentally in Ref. 13. Parametric amplification in a two-level atomic system in a resonant field was discussed in Refs. 14 and 15. Parametric amplification in sodium and barium vapor was produced ex-

perimentally in Refs. 11 and 16.

In this paper, we report an investigation of the susceptibility spectra of two-level systems in mono- and bichromatic fields, and the spectra of a three-level system in a monochromatic field. Data are presented on parametric generation in atomic vapor placed in the cavity of a dye laser.

2. THEORY

Susceptibility spectrum of a two-level system

When a two-level system is exposed to a monochromatic pump of frequency ω_1 (Fig. 1a), which is detuned from the resonance frequency ω_{21} by the amount $\Delta = \omega_1 - \omega_{21}$, the pump photons are scattered at frequencies $\omega_{3,4} = \omega_1 \pm \Omega'$, where $\Omega' = (\Delta^2 + \Omega_R^2)^{1/2}$ is the generalized Rabi frequency, $\Omega_R = 2|\mu_{21}E_1|/\hbar$ is the Rabi frequency, μ_{21} is the component of the matrix element of the transmission dipole moment along the direction of the electric field, and $2E_1$ is the amplitude of the electric field of the pump wave. Radiation at the anti-Stokes frequency $\omega_4 = \omega_1 + \Omega'$, close to ω_{21}, will then be absorbed, and radiation at the Stokes frequency $\omega_3 = \omega_1 - \Omega'$ will be amplified.[15] Amplification at the frequency ω_3 is due to three-photon stimulated Raman scattering, whereas amplification at ω_4 is possible because of the four-wave parametric process in the atomic medium.

A solution of the equation for the density matrix of a two-level system in a strong resonant pump field and a weak probe field was used in Refs. 4–7 to obtain an expression for the susceptibility $\chi^{(1)}(\omega_3)$ at the frequency ω_3 of the probe field:
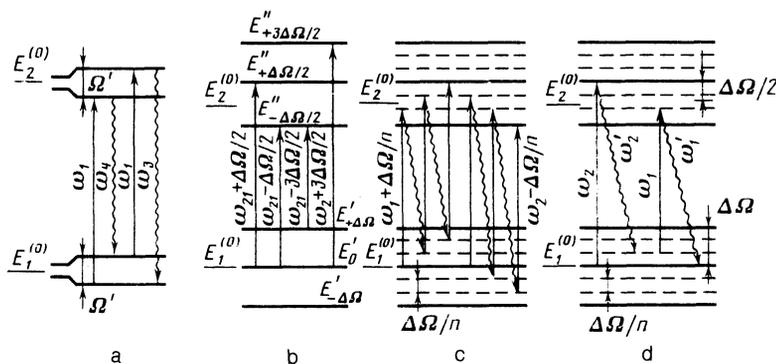

FIG. 1. Quasienergy-level scheme: a—each of the levels of the two-level system splits into two quasilevels in a strong light field of frequency ω_1, the two quasilevels being separated by Ω'; b—quasienergy levels formed from the two-level system and detuned by $\pm \Delta\Omega/2$ from the transition frequency ω_{21} in a bichromatic pump field; c—quasienergy levels in a bichromatic pump field corresponding to the absorption of three probe-field photons ($n = 3$); d—two-level system showing the absorption of two pump photons (ω_1 and ω_2) and the SRS of two photons at frequencies $\omega'_{1,2} = \omega_{1,2} \pm \Delta\Omega/3$ ($n = 3$).

$$\chi^{(1)}(\omega_3) = -\frac{N|\mu_{21}|^2(\rho_{22}-\rho_{11})^{(0)}}{\hbar D(\omega_3)}\left[\left(\omega_3-\omega_1+\frac{i}{T_1}\right)\right.$$
$$\times\left(\omega_3-2\omega_1+\omega_{21}+\frac{i}{T_2}\right)$$
$$\left.-\frac{2|\mu_{21}|^2|E_1|^2(\omega_3-\omega_1)}{\hbar^2(\omega_1-\omega_{21}-i/T_2)}\right], \qquad (1)$$

where $(\rho_{22}-\rho_{11})^{(0)}$ is the stationary population inversion produced by the pump field, given by

$$(\rho_{22}-\rho_{11})^{(0)} = \frac{[1+(\omega_1-\omega_{21})^2T_2^2](\rho_{22}-\rho_{11})_{t=0}}{1+(\omega_1-\omega_{21})^2T_2^2+4\hbar^{-2}|\mu_{21}|^2|E_1|^2T_1T_2}, \quad (2)$$

$$D(\omega_3)=(\omega_3-\omega_1+i/T_1)(\omega_3-\omega_{21}+i/T_2)(\omega_3$$
$$+\omega_{21}-2\omega_1+i/T_2)-4\hbar^2|\mu_{21}|^2|E_1|^2(\omega_3-\omega_1+i/T_2),$$

E_1 is the amplitude, ω_1 the frequency, and ω_{21} the transition frequency, T_1 and T_2 are the longitudinal and transverse relaxation times, and N is the atomic concentration.

Two-level system in a bichromatic pump field

Suppose that a two-level system with unperturbed level energies $E_1^{(0)}$ and $E_2^{(0)}$ experiences a "strong" field with amplitude E_1 and frequency ω_1 and a second strong field with the same amplitude E_1 and frequency ω_2. We shall assume that ω_2 and ω_1 differ by $\pm\Delta\Omega/2$ from the transition frequency ω_{21} and appear symmetrically in the spectrum $\Delta\Omega = \omega_2 - \omega_1$.

Using the time-dependent Schroedinger equation for the probability amplitudes $C_1(t)$ and $C_2(t)$, we can show that

$$idC_1/dt=F\cos(\Delta\Omega t/2)C_2,$$
$$idC_2/dt=F\cos(\Delta\Omega t/2)C_1, \qquad (3)$$

where

$$F=-|\mu_{21}|E_1/\hbar, \quad \omega_1=\omega_{21}-\Delta\Omega/2, \quad \omega_2=\omega_{21}+\Delta\Omega/2.$$

The set of equations given by (3) have the solution $[C_1(0) = 1, C_2(0) = 0]$

$$C_1(t)=\cos\xi(t), \quad C_2(t)=-i\sin\xi(t),$$

where

$$\xi(t)=2F\sin(\Delta\Omega t/2)/\Delta\Omega.$$

The coefficients $C_1(t)$ and $C_2(t)$ can be written in the form of expansions in terms of the Bessel functions:

$$C_1(t)=\sum_{m=-\infty}^{\infty}J_{2m}\left(\frac{2F}{\Delta\Omega}\right)\exp\left(i\cdot2m\frac{\Delta\Omega t}{2}\right),$$

$$C_2(t)=\sum_{m=-\infty}^{\infty}J_{2m+1}\left(\frac{2F}{\Delta\Omega}\right)\exp\left[i(2m+1)\frac{\Delta\Omega t}{2}\right], \qquad (4)$$

where $J_{2m}(2F/\Delta\Omega)$ and $J_{2m+1}(2F/\Delta\Omega)$ are Bessel functions of the first kind of order $2m$ and $2m+1$ ($m = 0,1,2...$), respectively. It follows from (4) that a set of quasienergy levels with energies

$$E_1'=E_1^{(0)}\pm2m\Delta\Omega/2,$$
$$E_2'=E_2^{(0)}\pm(2m+1)\Delta\Omega/2, \qquad (5)$$

where $m = 0,1,2,3,...$, is formed near each of the unperturbed levels with energies $E_1^{(0)}$ and $E_2^{(0)}$. The absorption

spectrum of the probe wave that corresponds to transitions between the quasilevels with energies E_1' and E_2' contains the frequencies

$$\omega'=\omega_{21}\pm(2k+1)\Delta\Omega/2, \qquad (6)$$

where $k = 0,1,2,...$. Figure 1b shows the set of quasienergy levels corresponding to (5). The vertical arrows indicate possible absorption lines.

Three-level system in the field of the pump wave

Studies of the change in the multiplet structure in a resonant light field are of considerable interest for both theoretical and experimental spectroscopy. Methods of calculating the quasienergy spectrum of an atom by time-dependent perturbation theory are presented in Ref. 17.

Consider the $3^2S_{1/2}$, $3^2P_{1/2}$, and $3^2P_{3/2}$ states of the sodium atom and suppose that a linearly polarized pump wave acts near the $3^2S_{1/2} - 3^2P_{1/2}(\omega_{12})$ and $3^2S_{1/2} - 3^2P_{3/2}(\omega_{13})$ transition frequencies. The selection rule $\Delta M = 0$ enables us to consider the set of energy levels of the sodium atoms as a three-level system. We assume in the calculation that the electron is in the ground state $S_{1/2}$ at $t = 0$. Under these conditions, the time-dependent Schroedinger equation yields the following set of equations for the probability amplitudes $C_1(t)$, $C_2(t)$, and $C_3(t)$:

$$idC_1/dt=C_2R_{12}\exp(i\delta_{12}t)+C_3R_{13}\exp(i\delta_{13}t),$$
$$idC_2/dt=C_1R_{12}\exp(-i\delta_{12}t),$$
$$idC_3/dt=C_1R_{13}\exp(-i\delta_{13}t), \qquad (7)$$

where

$$\delta_{12}=\omega_1-\omega_{21}, \quad \delta_{13}=\omega_1-\omega_{31},$$
$$R_{12}=-\mu_{12}E_1/2\hbar, \quad R_{13}=-\mu_{13}E_1/2\hbar,$$

and μ_{12} and μ_{13} are projections of the matrix elements of the dipole moments of the $S_{1/2} - P_{1/2}$ and $S_{1/2} - P_{3/2}$ transitions onto the polarization vector of the pump wave. The equations given by (7) are readily transformed [by substituting $Q_2 = C_2\exp(i\delta_{12}t)$ and $Q_3 = C_3\exp(i\delta_{13}t)$ into a set of equations with constant coefficients, whose solution enables us to find the energies of the quasienergy states:

$$E_{1,2,3}'=E_1^{(0)}+\hbar S_{1,2,3}, \quad E_{1,2,3}''=E_2^{(0)}+\hbar S_{1,2,3}+\hbar\delta_{12};$$
$$E_{1,2,3}'''=E_3^{(0)}+\hbar S_{1,2,3}+\hbar\delta_{13}, \qquad (8)$$

where $S_{1,2,3}$ are the roots of the characteristic equation

$$S^3+2\delta S^2+(\delta^2-\Delta^2/4-3R_{12}^2)S-(3\delta+\Delta/2)R_{12}^2=0, \qquad (9)$$

and

$$\delta=\omega_1-\overline{\omega}, \quad \Delta=\omega_{31}-\omega_{21}, \quad \overline{\omega}=(\omega_{21}+\omega_{31})/2.$$

The fact that $|\mu_{13}|^2 = 2|\mu_{12}|^2$ for transitions in the sodium atom was taken into account in the solution.

It follows from (8) that each of the three time-independent levels splits into three quasilevels, and only six of the quasienergy states have different energies. In the special case with $\delta = -\Delta/6$ we can readily find the roots of (9):

$$S_1=0, \quad S_{2,3}=\Delta/6\pm(\Delta^2/4+3R_{12}^2)^{1/2}. \qquad (10)$$

The absorption spectrum of the probe wave, corresponding to transitions between the quasilevels, then contains six absorption lines.

Amplification by the two-level system

A solution of the wave equation for the amplitudes $A_3(z)$ and $A_4^*(z)$ of waves propagating in a nonlinear medium (wave frequencies ω_3 and $\omega_4 = 2\omega_1 - \omega_3$) was obtained in Ref. 19 in the given-field approximation [constant field amplitude $A_1(z)$]. Since this condition was not satisfield in our experiments, we must repeat the calculations for coupled waves in a medium with varying $A_1(z)$, neglecting the reaction of the Stokes–anti-Stokes waves to the pump-wave amplitude:

$$\partial A_1/\partial z = -\alpha_1 A_1, \tag{11}$$

$$\partial A_3/\partial z = -\alpha_3 A_3 + K_3 A_4^* \exp(i\Delta k z), \tag{12}$$

$$\partial A_4^*/\partial z = -\alpha_4 A_4^* + K_4^* A_3 \exp(-i\Delta k z), \tag{13}$$

where Δk is the component of the vector difference ΔK along the z axis:

$$\Delta K = 2K_1 - K_3 - K_4, \tag{14}$$

$$\alpha_1 = -2\pi(\omega_1/n_1 c)\,\mathrm{Im}\,\chi^{(1)}(\omega_1, |E_1|),$$

$$\chi^{(1)}(\omega_1, |E_1|) = -N\mu_{12}\rho_{21}(\omega_1)/E_1, \tag{15}$$

$$\rho_{21}(\omega_1) = \mu_{21} E_1 (\rho_{22} - \rho_{11})^{(0)}/\hbar(\omega_1 - \omega_{21} + i/T_2), \tag{16}$$

$$\alpha_{3,4} = -2\pi(\omega_{3,4}/n_{3,4}c)\,\mathrm{Im}\,\chi^{(1)}(\omega_{3,4}, |E_1|), \tag{17}$$

where $\chi^{(1)}(\omega_{3,4}, |E_1|)$ is given by (1), $n_1, n_{3,4}$ are the refractive indices of the medium at frequencies ω_1, $\omega_{3,4}$, and

$$K_{3,4} = -2\pi i(\omega_{3,4}/n_{3,4}c)\chi^{(3)}(\omega_{3,4}, |E_1|)A_1^2, \tag{18}$$

$$\chi^{(3)}(\omega_3, |E_1|) = -N\mu_{12}\rho_{21}(\omega_3)/E_1^2 E_4^*. \tag{19}$$

In these expressions, $\chi^{(3)}(\omega_3 = 2\omega_1 - \omega_4)$ and $\chi^{(3)}(\omega_4 = 2\omega_1 - \omega_3)$ are the nonlinear susceptibilities that determine the parametric amplification of the waves and

$$\rho_{21}(\omega_s) = \frac{2\mu_{21}|\mu_{12}|^2 E_1^2 E_4^* (\rho_{22}-\rho_{11})^{(0)}(\omega_3-\omega_1+2i/T_2)}{\hbar^3 D(\omega_s)(\omega_1-\omega_{21}-i/T_2)}. \tag{20}$$

Using (14)–(16) subject to the condition

$$4\hbar^{-2}|\mu_{21}|^2|E_1|^2 T_1 T_2 \gg 1 + (\omega_1-\omega_{21})^2 T_2^2$$

we can reduce (11) to the form

$$A_1 \partial A_1/\partial z = -\alpha_1^{(0)}, \tag{21}$$

where

$$\alpha_1^{(0)} = \pi\omega_1 N\hbar/2n_1 c T_1.$$

Equation (21) is readily integrated:

$$A_1^2 = A_{10}^2 - 2\alpha_1^{(0)} z, \tag{22}$$

where $A_{10} = A_1(z=0)$ is the amplitude of the pump wave on the boundary of the nonlinear medium.

Let us consider the special case in which one of the waves, for example, the anti-Stokes wave, is amplified in the nonlinear medium much more than the Stokes wave. We then have $\partial A_3/\partial z = 0$ and we can use (12) to find the following expression for the amplitude A_3 (for $\Delta k = 0$):

$$A_3 = K_3^{(0)} A_1^2 A_4^*/\alpha_3, \tag{23}$$

where $K_3^{(0)} = K_3/A_1^2$. This expression is valid for α_3

$\gg |K_3^{(0)}||A_1^2|$, i.e., the nonlinear medium absorbs at the Stokes frequency ω_3. Substituting (22) and (23) in (13) and integrating, we find that (for $z_{\max} \ll A_{10}^2/2\alpha_1^{(0)}$ and neglecting the change in α_3, α_4 when the pump wave intensity is reduced)

$$A_4^* = A_{40}\exp(g_+ - 2K_3^{(0)}K_4^{(0)*}\alpha_1^{(0)}A_{10}^2 z/\alpha_3)z, \tag{24}$$

where $g_+ = -\alpha_4 + K_4^{(0)*}K_3^{(0)}A_{10}^4/\alpha_3$ is the gain and

$$K_4^{(0)*} = K_4^*/A_1^2, \quad A_{40} = A_4^*(z=0).$$

The solution we have obtained shows that the intensity of the anti-Stokes wave $(\sim|A_4|^2)$ increases exponentially during propagation in the nonlinear medium. The intensity reaches a maximum when the thickness is

$$z_a = g_+ \alpha_3/4K_3^{(0)}K_4^{(0)*}\alpha_1^{(0)}A_{10}^2 \tag{25}$$

and begins to decrease for $z > z_a$.

When $(z_{\max} \ll A_{10}^2/\alpha_1^{(0)})$, the solutions of (12) and (13) can be obtained in the given-field approximation [in (18), which determines $K_{3,4}$, $A_1^2 \equiv A_{10}^2$]:

$$A_3(z) = g_0^{-1}(K_3 - g_- - \alpha_3 - i\Delta k/2)A_0\exp(g_+ z) \times \exp(i\Delta k z/2), \tag{26}$$

$$A_4^*(z) = g_0^{-1}(K_4^* - g_- - \alpha_4 + i\Delta k/2)A_0\exp(g_+ z)\exp(-i\Delta k z/2),$$

where A_0 is the amplitude of the wave $A_3(z)$ and $A_4^*(z)$ on the boundary of the nonlinear medium at $z = 0$,

$$g_\pm = \pm\tfrac{1}{2}[(\alpha_3-\alpha_4+i\Delta k)^2+4K_3 K_4^*]^{1/2} - \tfrac{1}{2}(\alpha_3+\alpha_4), \tag{27}$$

$$g_0 = g_+ - g_-, \quad \alpha_{3,4} = \alpha_{3,4}'' - \alpha_{3,4}', \tag{28}$$

$$\alpha_3' = \frac{4\pi|\mu_{21}|^4 N\omega_3|E_1|^2}{n_3 c\hbar}\,\mathrm{Im}\,\frac{(\omega_3-\omega_1)(\rho_{22}-\rho_{11})^{(0)}}{D(\omega_3)(\omega_1-\omega_{21}-i/T_2)}, \tag{29}$$

$$\alpha_3'' = \frac{2\pi|\mu_{21}|^2 N\omega_3}{n_3 c\hbar}$$
$$\times \mathrm{Im}\,\frac{(\omega_3-\omega_1+i/T_1)(\omega_3-2\omega_1+\omega_{21}+i/T_2)(\rho_{22}-\rho_{11})^{(0)}}{D(\omega_3)}, \tag{30}$$

α_3' is the gain at frequency ω_3, due to three-photon stimulated Raman scattering, and α_3'' is the absorption coefficient at the frequency ω_3. The values of α_4' and α_4'' can be obtained from (29) and (30) by replacing ω_3 with ω_4.

The expressions given by (26)–(30) show that the intensities of the waves coupled parametrically in the nonlinear medium at frequencies ω_3 and ω_4 increase exponentially, and the total gain is

$$g_+ = g_0/2 + \alpha_0' - \alpha_0'', \tag{31}$$

where

$$\alpha_0'' = (\alpha_3''+\alpha_4'')/2, \quad \alpha_0' = (\alpha_3'+\alpha_4')/2,$$

$g_0/2$ is the gain determined by the four-wave parametric processes in the nonlinear medium, α_0' is the gain determined by the three-photon stimulated Raman scattering, and α_0'' is the absorption coefficient reduced by saturation.

The expressions given by (26) describe exponentially growing Stokes and anti-Stokes intensities and are valid when

$$z|(\alpha_3-\alpha_4+i\Delta k)^2+4K_3 K_4^*|^{1/2} \gg 1.$$

Let us consider some special cases.

(1) When $|E_1|^2 = 0$ the expressions given by (26) describe the Bouguer law $(g_+ = -\alpha_3'' = -\alpha_4'')$

$$\alpha_3'' = \frac{2\pi|\mu_{21}|^2 N\omega_3}{n_3 c\hbar} \frac{T_2}{(\omega_3-\omega_{21})^2 T_2^2+1}. \tag{32}$$

This is the usual Lorentz absorption line profile.

(2) At precise resonance $\omega_1 = \omega_{21}$, we can show from (17) that $\alpha_3 = \alpha_4 = \alpha_0$ and

$$g_\pm = -\alpha_0 \pm {}^1\!/_2 (4K_3 K_4^* - \Delta k^2)^{1/2}.$$

When $|K_3| \gg |\Delta k|$, and since $\operatorname{Re} K_3 = -\operatorname{Re} K_4 = \varkappa$ and $\operatorname{Im} K_3 = \operatorname{Im} K_4 = \beta$, we have

$$g_\pm = -\alpha_0 \pm (i\varkappa + \beta). \tag{33}$$

(3) When $\omega_1 - \omega_{21} \gg T_2^{-1}$ is satisfied, we can show that $K_3, K_4 \gg \alpha_3, \alpha_4$. We then have

$$\chi^{(3)}(2\omega_1-\omega_4) = \chi^{(3)}(2\omega_1-\omega_3)$$

$$= \frac{2\hbar^{-3}N|\mu_{21}|^4 (\rho_{22}-\rho_{11})^{(0)}}{(\omega_1-\omega_{21})(\omega_3-\omega_{21})(\omega_4-\omega_{21})}. \tag{34}$$

and

$$|K_3| = |K_4|, \quad g_+ = -g_- = |K_3^{(0)}| = |K_4^{(0)}| \gg 1,$$

$$|A_3| = |A_4| = A_{10} \exp(|K_3^{(0)}|z). \tag{35}$$

Thus, in experiments with large enough detuning from resonance, the gain g_+ is determined by the four-wave parametric process, which requires that the phase-locking conditions be satisfied. This is in contrast to the case of gain due to three-photon stimulated Raman scattering, which does not require phase-locking.

Parametric amplification in cases (2) and (3) should lead to generation at frequencies ω_3 and ω_4, where $\omega_{3,4} = \omega_1 \pm \Omega'$ and Ω' is the generalized Rabi frequency. It is useful to consider the following numerical estimates: $\omega_1 - \omega_{21} = 100\ T_2^{-1}$, $N = 10^{17}$ cm^{-3}, $T_1 = 9 \cdot 10^{-9}$ sec, $T_2 = 7 \cdot 10^{-12}$ sec, $|K_3| \approx 4$ cm^{-1}, $|\mu_{12}| = 1.5 \cdot 10^{-17}$ cgs, $E_1 = 1.2 \cdot 10^2$ cgs, $\alpha_3' - \alpha_3'' = 0.8$ cm^{-1}, $|\Delta k| = 0.004$ cm^{-1}, $g_+ \approx 4.8$ cm^{-1}.

(4) The phase-locking condition $\Delta k = 0$ is satisfied for the angle between the wave vectors $\mathbf{K}_1$ and $\mathbf{K}_3$, given by

$$\theta = [\omega_3(n_3\omega_3+n_4\omega_4-2\omega_1 n_1)/\omega_1\omega_4]^{1/2}, \tag{36}$$

where n_1, n_3, n_4 are the refractive indices at frequencies $\omega_1, \omega_3, \omega_4$.

When the concentration of atoms is $N = 0.8 \times 10^{17} - 2 \times 10^{17}$ cm^{-3}, $T_1 = 8.5$ ns, $T_2 = 4$ ps, $|\mu_{21}| = 6 \times 10^{-18}$ cgs, and the detuning from resonance $\omega_1 - \omega_{21}$ is up to $10 T_2^{-1}$, the angle lies in the range 0.7–1.2° and, in the case of precise resonance $(\omega_1 = \omega_{21})$, the phase-locking condition is practically satisfied for the collinear propagation of all three beams $(\theta \sim 0.1')$.

When $\theta \gg 2°$, the waves are not parametrically coupled and

$$|A_3| = A_{10} \exp[(\alpha_3'-\alpha_3'')z].$$

The amplification factor α_3' for the Stokes wave is then entirely determined by three-proton stimulated Raman scattering. According to Ref. 15, in the direction of exact phase-

locking ($\Delta k = 0$), there is no amplification of the probes waves at frequencies $\omega_{3,4} = \omega_{21} \mp \Omega'$. However, the amplification maxima for the waves $A_3(z)$ and $A_4^*(z)$ at these frequencies correspond to the directions of propagation lying close to the direction of phase-locking $|\Delta k/\alpha_0| < 0.1$, where $\alpha_0 = 4\pi N\omega_{21}|\mu_{21}|^2 T^2/\hbar c$ is the absorption coefficient.

3. EXPERIMENTAL RESULTS
Susceptibility spectrum of barium atoms (two-level system) in monochromatic and bichromatic fields

We shall now present experimental results on the susceptibility spectrum of barium atoms near the resonance transition $6^1S_0-6^1P_1$ ($\lambda = 553.5$ nm) which constitutes a "good" two-level system. We investigated the susceptibility spectrum in monochromatic and bichromatic pump fields, using wide-band probe radiation and holographic interference spectroscopy (Refs. 11 and 18).

Figure 2 shows a block diagram of the apparatus employed. The atomic barium vapor was produced by evaporation and dissociation of barium hydroxide in an ac arc discharge (current ~ 10 A). The length of the absorbing layer in the gap between the electrodes was 5–10 mm. The barium vapor 10 was placed in one of the arms of a Michelson interferometer consisting of the beam-splitting cube 9 and mirrors 11 and 12. The strong narrow-band pump radiation ($\Delta\lambda \approx 0.05$ nm) was produced by a dye laser whose cavity was formed by mirrors 5, 7 and diffraction grating 6 mounted at a glancing angle of about 85°. The low-intensity probe radiation ($\Delta\lambda \sim 10$–20 nm) was produced by a coupled cavity of the same dye laser, formed by mirror 5 and glass plate 8, mounted in the zero order of the diffraction grating 6.

The dye laser was pumped by the second-harmonic radiation from the ruby laser 1 (output power ~ 400–800 kW, pulse length ~ 30 ns), generated after the KDP crystal 2. The second harmonic radiation was focused by cylindrical lens 3 in the quartz cell 4 containing the dye (coumarin 153) with windows cut at the Brewster angle. This cell, the mirrors 5, 7, and 8, and the grating 6 formed a laser with two
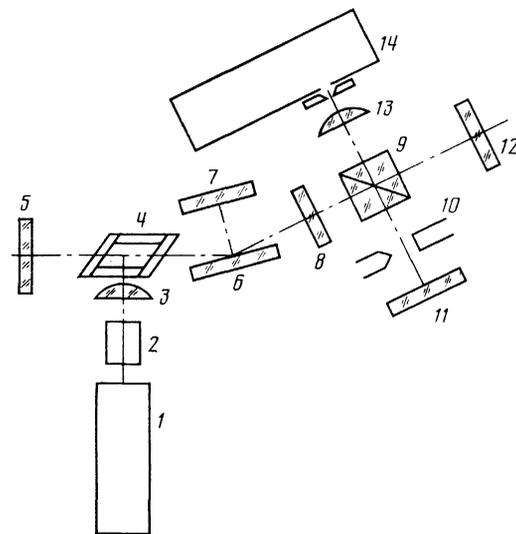

FIG. 2. Block diagram of apparatus: 1—ruby laser; 2—KDP crystal; 3, 13—cylindrical lenses; 4—cell containing the dye (rhodamine 6G or coumarin 153); 5—90% mirror; 6—diffraction grating; 7—100% mirror; 8—plane-parallel plate; 9—beam-splitting cube; 10—arc discharge (IBS-28); 11, 12—100% mirrors; 14—spectrograph.
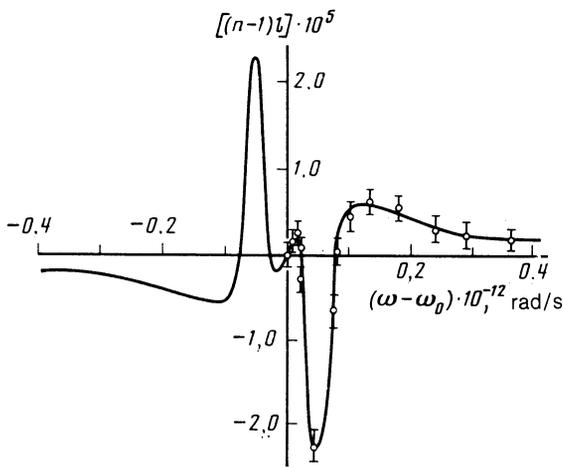
FIG. 3. Refractive index spectrum of the two-level system in a resonant light field. Points—experimental; solid curve—theoretical[4]; l—thickness of absorbing layer.

coupled cavities. After the interferometer 9–12, the beam from the dye laser was focused by the cylindrical lens 13 in the plane of the exit slit of spectrograph 14 (reciprocal linear dispersion of about 0.26 nm/mm). Spectroholograms with fringe frequency of about 10 lines/mm were produced in the exit plane of the spectrograph 14 when a path difference of about 12 mm was introduced between the two arms of the Michelson interferometer.

Monochromatic pump

The narrow-band radiation produced by the dye laser was tuned to resonance with the 6^1S_0–6^1S_1 transition frequency, and the wide-band radiation field was used as the probe beam. The pump power density was about 5×10^6 W/cm^2, and that of the probe field was lower by two orders of magnitude. Interferograms were produced by illuminating the spectrohologram with a plane wave from a helium–neon laser and using interference in diffraction orders ± 1. The interference fringes on this interferogram were arranged to be perpendicular to the absorption lines. Near an absorption line, the fringes reflect the behavior of the refractive index

$$n_3 - 1 = 2\pi \, \mathrm{Re}\, \chi^{(1)}(\omega_3), \qquad (37)$$

on a particular scale, where $\chi^{(1)}(\omega_3)$ is given by (1).

Figure 3 shows the result of an analysis of the interferogram. The spread of the experimental points corresponds to the spread of the interference fringes along the vertical axis of the pattern. The experimental points corresponding to extrema and zeros were then used with (1) to determine the

unknown parameters and to construct the theoretical dependence of $(n_3 - 1)l$ on $\omega_3 - \omega_1$. The parameters deduced from the experimental results were as follows: $\Gamma_1 = 0.74 \cdot 10^9$ rad/s ($\Gamma_1 = 2\pi T_1^{-1}$, $T_1 = 8.5$ ns is the lifetime of the state 6^1P_1, $f = 1.4$) and $\Gamma_2 = 0.3 \cdot 10^{12}$ rad/s ($\Gamma_2 = \pi T_2^{-1}$).

The Rabi frequency, determined from the size of the splitting, was $\Omega_R = 1.8 \cdot 10^{12}$ rad/s. The value $E_1 = 1.2 \cdot 10^2$ cgs was then calculated from this frequency for $|\mu_{12}| = 1.5 \cdot 10^{-17}$ cgs. It is clear from Fig. 3 that the theoretical graph fits quite well the experimental points. The product Nl was determined from the experimental results $(n_3 - 1)l = 2.2 \cdot 10^{-5}$, using (1)–(3). The result obtained for the above parameters was $(Nl)_{\mathrm{calc}} \approx 9 \cdot 10^{17}$ cm^{-2}. It is shown in Ref. 19 that four-photon processes involved in the parametric interaction of the waves with frequencies ω_3 and ω_4 could be neglected in an optically thin layer.

Bichromatic pumps

The bichromatic and probe radiations were produced with basically the same dye laser arrangement as in Fig. 2. The second frequency of the high-intensity pump field was generated by mounting the diffraction grating 6 in a Litthrow scheme so that it formed an autocollimating cavity with the 90% mirror 5 in the third order of the diffraction grating. The frequency spectrum of the generated bichromatic pump field could be scanned by rotating mirror 7 and grating 6. The dye laser radiation produced in this way was directed into the Michelson interferometer 9–12 containing the atomic medium 10 in one of its arms. The frequencies of the bichromatic pump field were arranged symmetrically relative to the barium resonance line ($\lambda = 553.5$ nm) with a detuning of ± 0.4 nm.

Figure 4a shows the interferogram obtained using the spectrohologram with a posteriori processing and an increase in the sensitivity coefficient by a factor of 8. The interference fringes reproduce on a certain scale the refractive index spectrum and, in addition, the interferogram visualizes the absorption lines. It is clear that new absorption lines (subharmonics) have appeared in the biharmonic field and "converge" to the frequencies ω_1 and ω_2 of the pump field, in accordance with the law $\omega'_{1,2} = \omega_{1,2} \pm \Delta\Omega/n$ where $\Delta\Omega = \omega_2 - \omega_1$, $n = 1,2...$. Weak-field gain resonances were observed between the absorption resonances.

To explain the apearance of the subharmonics in the absorption spectrum of the probe fields, we must consider the time dependence of the absorption coefficient $k_\omega(t)$ of the probe radiation. When $\Delta\Omega \gg |F|$, it follows from (4) that $(k_\omega(t) \propto |C_2(t)|^2)$

$$k_\omega(t) \propto (2F/\Delta\Omega)^2 (1 - \cos \Delta\Omega t). \qquad (38)$$
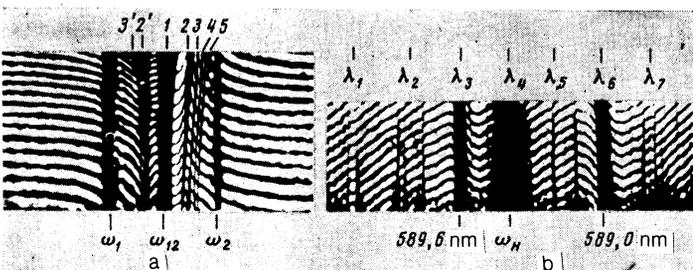

FIG. 4. a—Interferogram of quasiresonant bichromatic light fields (ω_1 and ω_2) near the $\lambda = 553.5$ nm line (ω_{12}), 2–5 and 2', 3'—absorption subharmonics; b—interferogram arranged to show the "hooks" for a detuning of the strong field by 0.2 nm from $\lambda = 589.6$ nm.

2438   Sov. Phys. JETP 67 (12), December 1988
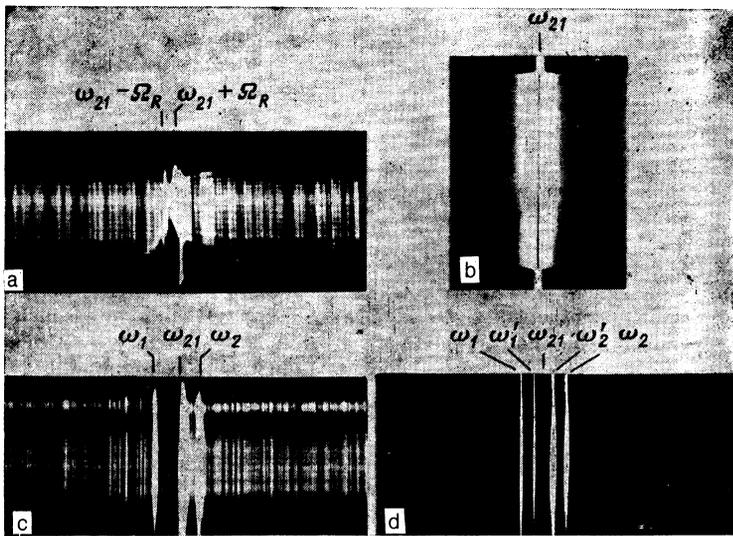
Zeĭlikovich et al.   2438

FIG. 5. Two-level system in a light field: a—amplification spectrum in the field of the monochromatic wave; b—generation spectrum in the field of the monochromatic pump; c, d—generation spectrum in the field of the biharmonic pump (ω_1 and ω_2) at frequencies $\omega_{1,2} \pm \Delta\Omega/2$ and $\omega_{1,2} \pm \Delta\Omega/3$.

This shows that the absorption coefficient of the low-intensity field is modulated in time with the period $T_n = 2\pi n/\Delta\Omega$. For $n = 1$, one weak-field photon is absorbed, and $n = 2,3,...$ correspond to two-photon, three-photon, etc., resonances. In the energy representation, this corresponds to the following interval of possible absorption frequencies: $\Delta\omega_n = \Delta\Omega/n$. Figure 1c illustrates the quasienergy level scheme for the atom in the field of the bichromatic pump. The vertical lines show the absorption of probe-field photons for $n = 3$.

Susceptibility spectrum of sodium atoms (three-level system)

We shall now present the experimental results on the susceptibility spectrum corresponding to the first doublet of the sodium atom in a resonant linearly polarized pump field. In our experiments, the strength of the interaction between the system and the field was comparable with the spin-orbit interaction, and we again used holographic interference spectroscopy. The block diagram of the apparatus was the same as that shown in Fig. 2. However, the Michelson interferometer was replaced with the Mach-Zender interferometer. The cell ($l \approx 20$ cm) containing the sodium vapor inserted into one of the arms of the latter. The cell was heated to about 180 °C (sodium atom concentration $\approx 5 \times 10^{11}$ cm^{-3}). The narrow-band dye laser radiation was tuned to a frequency close to the $3^2S_{1/2}$–$3^2P_{1/2}$ transition frequency and the broad-band radiation was used as the probe beam. Illumination of the spectrohologram by a plane wave from a helium-neon laser and interference of diffraction orders ± 1 produced the required interferograms, one of which, showing the characteristic "hooks," is reproduced in Fig. 4b. The pump power density was 5×10^6 W/cm^2 and the corresponding figure for the probe beam was lower by two orders of magnitude. Figure 4b shows the refractive index spectrum, in which the theoretically predicted positions of seven absorption lines are indicated by $\lambda_1 - \lambda_7$, where λ_4 is the pump wavelength. These lines should be observed in the spectrum when the monochromatic pump field is introduced with a detuning $\delta_{12} = 0.2$ nm from the long-wave absorption line ω_{12}. The bifurcation of the absorption lines λ_1, λ_2 and λ_5 is probably due to the wavelength spread of the pump field ($\Delta\lambda \approx 0.05$ nm).

Parametric amplification and generation in atoms

We investigated the amplification spectrum outside the dye laser cavity for atomic barium vapor in an arc discharge in a monochromatic pump field. Figure 5a is a photograph of the amplification spectrum ($\omega_1 = \omega_{21}$). The photograph clearly shows narrow-band amplification regions shifted by the Rabi frequencies ($\omega_{21} \pm \Omega_R$), where $\Omega_R \approx 1.2 \cdot 10^{12}$ rad/s. Moreover, there is a subfocus region in the spectrum of the probe radiation (for $\omega_3 > \omega_{21}$) that is characterized by a vertical compression of the spectrum, which is produced by the nonlinear frequency-dependent lens induced in the atomic medium. The spectrum of the probe radiation is expanded along its height for $\omega_3 < \omega_{21}$ by the negative frequency-dependent lens induced in the atomic medium by the resonant pump field. These experiments confirm the theoretical model put forward in Ref. 11.

We have also measured the maximum gain by photometering the spectrum of the amplification line and of the probe radiation near the amplification line. The maximum total gain per transit was found to depend on the particular experimental conditions and lay in the range $g_+/2 \approx 2$–5 cm^{-1}. The length of the absorption layer was $l = 0.5$ cm. These experiments were performed with the following parameter values: $\Omega_R = 1.8 \cdot 10^{12}$ rad/s (determined from the magnitude of the splitting), $\Gamma_2 = 0.8 \cdot 10^{12}$ rad/s (determined from the line halfwidth), and $N = 0.5 \times 10^{17} - 10^{17}$ cm^{-3}. The values calculated from (24)–(27) were: $\alpha'_3 - \alpha''_3 = 1$–$2$ cm^{-1} and $g_0/2 = 2.5$–5 cm^{-1}. The total gain was $g_+ = 3.5$–7 cm^{-1} and was thus mainly determined by the parametric four-wave interaction.

Generation at the Rabi frequencies ($\omega_{21} \pm \Omega_R$) was produced[20] when the arc discharge in the barium vapor was initiated in the dye-laser cavity between mirror 5 and cell 4 (Fig. 2). The narrow-band pump radiation was tuned to resonance with the 6^1S_0–6^1P_1 ($\lambda = 553.5$ nm) transition. The spectrum of the radiation produced by the dye laser is shown in Fig. 5b. We note that the separation between the generated frequencies was changed when the pump intensity was altered.

Generation at frequencies $\omega_{1,2} \pm \Delta\Omega/2$ and $\omega_{1,2} \pm \Delta\Omega/3$ was observed (Figs. 5c and d) when the barium vapor was placed in the cavity of the two-frequency dye la-

ser. It was probably due to the four-wave parametric interaction between the two waves of the bichromatic pump field (ω_1 and ω_2) and the two waves (ω_1') and ω_2' produced by stimulated Raman scattering. Figure 1d demonstrates four-photon stimulated Raman scattering in which two photons of the pump field with frequencies ω_1 and ω_2 are absorbed and two photons are scattered at frequencies $\omega_1' = \omega_1 + \Delta\Omega/3$ and $\omega_2' = \omega_2 - \Delta\Omega/3$. Figure 5c shows the spectrum generated at the frequency $\omega_2' = \omega_1' = \omega_{1,2} \pm \Delta\Omega/2$, and Fig. 5d reproduces the spectrum at frequencies $\omega_2' = \omega_2 - \Delta\Omega/3$ and $\omega_1' = \omega_1' + \Delta\Omega/3$. In this case, we have a transfer of energy from the pump-field components to the scattered-field components.

One of the pump waves, e.g., the wave of frequency ω_2, interacts with the SRS Stokes wave (frequency $\omega_1' = \omega_1 + \Delta\Omega/n$) and produces a nonlinear polarization wave of frequency $\omega_2 - \omega_1'$ in the atomic medium. The other pump wave, ω_1, interacts with the nonlinear polarization wave. This produces wave amplification at the anti-Stokes frequency

$$\omega_2' = \omega_1 + \omega_2 - \omega_1' = \omega_2 - \Delta\Omega/n.$$

The interacting waves must then satisfy the condition

$$|(\mathbf{K}_1 + \mathbf{K}_2 - \mathbf{K}_1' - \mathbf{K}_2')_z/\alpha_0| < 0,1,$$

where $\mathbf{K}_1$ and $\mathbf{K}_2$ are the pump-wave vectors and $\mathbf{K}_1'$ and $\mathbf{K}_2'$ the wave vectors of the SRS waves.

We also investigated amplification in the three-level system. Generation was produced by introducing sodium vapor into the dye-laser cavity by evaporating and dissociating NaCl in the ac discharge (current ≈ 4 A). The thickness of the absorbing layer in the space between the electrodes was ≈ 5 mm. The pump power density (ω_1) in the cavity was $\approx 10^7$ W/cm^2.

Figure 6 shows the generation spectra for different detunings $\omega_1 - \omega_2$ of the narrow-band line. It is clear that the spectrum contains a new emission line whose frequency (ω_a in Figs. 6a and c and ω_c in Fig. 6b) depends on the frequency of the narrow-band pump radiation $\omega_1 - \omega_{21}$. It is important to note that the coefficient describing the conversion of the pump wave into radiation at the new frequency is quite high. For example, in Fig. 6a, the radiation of frequency ω_1 is almost completely transformed into radiation of frequency ω_a.

Figures 7b–d show the positions of quasilevels calculated from (8) for cases corresponding to the spectra of Fig. 6a–c. All the quantities, with the exception of R_{12}^2, necessary for calculations based on (8), are readily determined from the experimental results shown in Fig. 6. Computer simulations were used to determine R_{12} together with the electric field E_1 in the expression for R_{12}. Thus, for the experiment illustrated in Fig. 6a, we found that $E_1 \approx 5 \cdot 10^4$ V/cm, whereas, for the experiment of Fig. 6b, $E_1 \approx 10 \cdot 10^4$ V/cm. Finally, the value corresponding to the experiments of Fig. 6c is $E_1 \approx 9 \cdot 10^4$ V/cm. We also estimated the field strength from the power density, and this yielded $E_1 \approx 8 \cdot 10^4$ V/cm, which is in good agreement with the calculations.

The mechanism responsible for generation at the frequencies shown in Fig. 7b–d requires further examination. However, it is important to note that, in the case of amplification at the anti-Stokes frequency (Fig. 6a–c), the amplifi-

FIG. 6. Generation spectra for different detuning $\omega_1 - \omega_{21}$ of the narrow-band line; ω_{31} ($\lambda = 589.0$ nm) and ω_{21} ($\lambda = 589.6$ nm)—reference lines produced by a sodium lamp; ω_1—narrow-band pump radiation; ω_c, ω_a—generation lines that appear when sodium atoms are introduced into the cavity.

cation mechanism was, in our view, the parametric four-wave interaction.

The scattering of a high-intensity wave of frequency ω_1 is accompanied by the emission of photons at the Stokes frequency ω_c. The Stokes wave interacts with the high-intensity wave (ω_1) and creates a nonlinear polarization wave of frequency $\omega_1 - \omega_c$ in the atomic medium. When the high-intensity pump wave of frequency ω_1 interacts with the nonlinear polarization wave, this creates a new wave of frequency.

$$\omega_a = 2\omega_1 - \omega_c.$$

This is confirmed by the increase in the angular size of the generation line (at frequency ω_a) as compared with the pump wave (ω_1) in Fig. 6a.

The following condition must be satisfied in parametric four-wave amplification if energy is to be efficiently transferred from the field of frequency ω_1 to radiation at frequency ω_a:

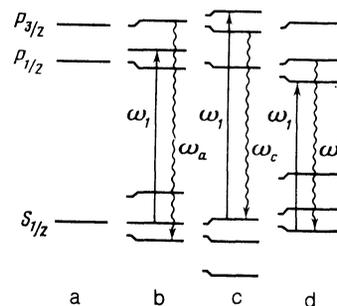$$|(\mathbf{K}_a - 2\mathbf{K}_1 + \mathbf{K}_c)_z/\alpha_0| < 0,1,$$

FIG. 7. Level scheme for sodium in the absence of the external field (a) and the quasilevel scheme produced by the narrow-band pump radiation ω_1 (b–d); ω_a, ω_c—transitions between quasilevels that correspond to the observed generation.

where $\mathbf{K}_a, \mathbf{K}_1, \mathbf{K}_c$ are the wave vectors corresponding to the three frequencies. The phase-locking condition is satisfied for the propagation of the anti-Stokes component at an angle θ to the direction of the pump wave ω_1. The angle θ can be determined from (36). Generation of the Stokes component (Fig. 6b) can probably be explained by three-photon SRS.

CONCLUSION

1. Amplification and generation spectra produced in a vapor of two-level atoms (barium) in a monochromatic pump field were investigated theoretically and experimentally. The total intensity gain was determined $(4\text{--}10 \text{ cm}^{-1})$ at the Rabi frequency $\Omega_R = 1.8 \cdot 10^{12} \text{ rad/s}$.

2. The absorption spectra of a vapor of two-level atoms (barium) in the field of a bichromatic pump was investigated theoretically and experimentally for a symmetric detuning of the pump wave frequencies from the resonance transition frequency (detuning by ± 0.4 nm from the resonance wavelength $\lambda = 553.5$ nm). The spectrum was found to contain new absorption lines (subharmonics) which converged to the frequencies ω_1 and ω_2 of the pump waves in accordance with the law $\omega'_{1,2} = \omega_{1,2} \pm \Delta\Omega/n$, where $\Delta\Omega = \omega_2 - \omega_1$ $(n = 1,2...)$. Amplification resonances were observed between absorption resonances for the weak field. When the barium vapor was located in the cavity of a two-frequency dye laser, generation was produced at the frequencies $\omega_{1,2} \pm \Delta\Omega/2$ and $\omega_{1,2} \pm \Delta\Omega/3$.

The absorption spectra of the vapor of three-level atoms (sodium) in a monochromatic pump were investigated theoretically and experimentally. Six absorption lines were found and their positions were in agreement with theoretical calculations. When sodium vapor was introduced into the laser cavity, generation was observed at frequencies corresponding to those of transitions between quasilevels.

[1]S. G. Rautian and I. I. Sobel'man, Zh. Eksp. Teor. Fiz. 41, 456 (1961); 44, 934 (1963) [Sov. Phys. JETP 14, 328 (1962); 17, 424 (1963)].
[2]P. A. Ananasevich, Opt. Spektrosk. 14, 612 (1963); 16, 709 (1964) [Opt. Spectrosc. (USSR) 14 (1963); 16 (1964)].
[3]T. I. Kuznetsova and S. G. Rautian, Zh. Eksp. Teor. Fiz. 49, 1605 (1965) [Sov. Phys. JETP 22, 1098 (1966)].
[4]P. A. Ananasevich, Dokl. Akad. Nauk BSSR 12, 878 (1968).
[5]P. A. Ananasevich, Fundamentals of the Theory of Interaction of Light With Matter [in Russian], Nauka i Tekhnika, Minsk, 1977.
[6]B. R. Mollow, Phys. Rev. A 5, 2217 (1972).
[7]D. J. Harter and R. W. Boyd, IEEE J. Quantum Electron QE-16, 1126 (1980).
[8]D. N. Klyshko, Yu. S. Konstantinov, and V. S. Tumanov, Izv. Vyssh. Uchebn. Zaved. Radiofiz. 8, 513 (1965).
[9]A. M. Bonch-Bruevich, V. A. Khodovoi, and N. A. Chigir', Zh. Eksp. Teor. Fiz. 67, 2069 (1974) [Sov. Phys. JETP 40, 1027 (1975)].
[10]E. Y. Wu, S. Ezekiel, M. Ducloy, et al., Phys. Rev. Lett. 38, 1077 (1977).
[11]I. S. Zeilikovich, S. A. Pul'kin, and L. S. Gaida, Zh. Eksp. Teor. Fiz. 87, 125 (1984) [Sov. Phys. JETP 60, 72 (1984)].
[12]R. Y. Chiao, P. L. Kelley, and E. Garmire, Phys. Rev. Lett. 17, 1158 (1966).
[13]R. L. Carman, R. Y. Chiao, and P. L. Kelley, Phys. Rev. Lett. 17, 1281 (1966).
[14]B. R. Mollow, Phys. Rev. A 7, 1319 (1973).
[15]R. W. Boyd, M. G. Raymer, P. Narum, et al., Phys. Rev. A 24, 411 (1981).
[16]D. J. Harter, P. Narum, M. G. Raymer, et al., Phys. Rev. Lett. 46, 1192 (1981).
[17]B. A. Zon and B. G. Katsnel'son, Zh. Eksp. Teor. Fiz. 65, 947 (1973) [Sov. Phys. JETP 38, 470 (1974)].
[18]I. S. Zeilkovich and S. A. Pul'kin, Opt. Spektrosk. 53, 588 (1982) [Opt. Spectrosc. (USSR) 53, 349 (1982)].
[19]S. R. Zeiger, Theoretical Foundations of Laser Saturation Spectroscopy [in Russian], Leningrad State University, 1979, p. 165.
[20]I. S. Zeilikovich, S. A. Shul'kin, and L. S. Gaida, Opt. Spektrosk. 62, 1401 (1987) [Opt. Spectrosc. (USSR) 62, 827 (1987)].

Translated by S. Chomet